A facile hydrothermal synthesis, characterization and magnetic properties of mesoporous $CoFe_2O_4$ nanospheres

M. Penchal Reddy [a,*], A.M.A. Mohamed [a,b], X.B. Zhou [c], S. Du [c], Q. Huang [c]

[a] Center for Advanced Materials, Qatar University, Doha 2713, Qatar
[b] Department of Metallurgical and Materials Engineering, Faculty of Petroleum and Mining Engineering, Suez University, Suez 4372, Egypt
[c] Ningbo Institute of Materials Technology and Engineering (NIMTE), Chinese Academy of Sciences (CAS), Ningbo 315201, Zhejiang, RP China

ARTICLE INFO

Keywords:
$CoFe_2O_4$
Hydrothermal method
Porous nanospheres
Magnetic properties
XPS

ABSTRACT

Mesoporous $CoFe_2O_4$ nanospheres with an average size of 180 nm were fabricated via a facile hydrothermal process using ethylene glycol as solvent and sodium acetate (NaAc) as electrostatic stabilizer. In this method, ethylene glycol plays a vital role in the formation of cobalt nanoospheres as a solvent and reducing agent. The structure and morphology of the prepared materials were characterized by X-ray diffraction (XRD), scanning electron microscopy (SEM), transmission electron microscopy (TEM), high-resolution TEM (HRTEM), Fourier transform infrared spectroscopy (FTIR) and X-ray photoelectron spectroscopy (XPS). The nanospheres exhibited ferromagnetic properties with high saturation magnetization value of about 60.19 emu/g at room temperature. The BET surface area of the nanospheres was determined using the nitrogen absorption method. The porous $CoFe_2O_4$ nanospheres displayed good magnetic properties, which may provide a very promising candidate for their applications in target drug delivery.

1. Introduction

Mesoporous materials have a high surface area, uniform and tunable pore sizes, and various morphologies and compositions, which favor their applications in various fields such as catalysis, energy, optics, medicine, electronics and biotechnology [1–5]. The cubic spinel structured ferrite MFe_2O_4, represents a well-known and important class of iron oxide materials. In these materials, oxygen forms a face-centered cubic (fcc) close packing, and the tetrahedral (A) and octahedral (B) sites are occupied by the Fe^{3+} ions and the divalent metal ions (M^{2+}), respectively. Among the spinel ferrites, cobalt ferrite ($CoFe_2O_4$), a well-known hard magnetic material, has been extensively studied because of its interesting magnetic properties. The moderate saturation magnetization, large magneto-crystalline anisotropy, high coercivity, chemical stability and mechanical hardness make the cobalt ferrite as one of the competitive candidates for high-density magnetic recording media [6,7]. Therefore research on development of fabrication methods for ferrite nanoparticles with desirable magnetic property, acceptable chemical stability and surface chemistry that allow attracting interest of several research groups for straight forward functionalization with different surface active motives.

Recently, solvothermal method has been successfully used to fabricate $MgFe_2O_4$, $MnFe_2O_4$ and $NiFe_2O_4$ nano/microspheres [8–10]. For high performance in function-specific biological applications, magnetic particles must be spherical with smooth surfaces, narrow size distributions, large surface areas, high magnetic saturation to provide maximum signal, and good dispersion in liquid media [11–13]. Owing to the great application potentials in catalysis, adsorption, separation, mesoporous magnetic nanospheres have been of keen interest recently. Herein, the aim of the present work was undertaken to report in details the hydrothermal synthesis, characterization, and magnetic properties of mesoporous spinel $CoFe_2O_4$ nanospheres.

2. Experimental procedure

All chemicals were of analytic grade and used as received without further purification. The mesoporous ferrite nanospheres were prepared via a hydrothermal reaction in ethylene glycol. In a typical experiment, 2.5 mmol $CoCl_2 \cdot 6H_2O$ and 5 mmol $FeCl_3 \cdot 6H_2O$ were dissolved in 40.0 mL ethylene glycol ($HOCH_2CH_2OH$). 3.6 g of sodium acetate trihydrate ($CH_3COONa \cdot 3H_2O$) and 2 g of polyethylene glycol (PEG-4000) was added under magnetic stirring. This mixture was then

* Corresponding author.
E-mail address: reddy@nimte.ac.cn (M.P. Reddy).

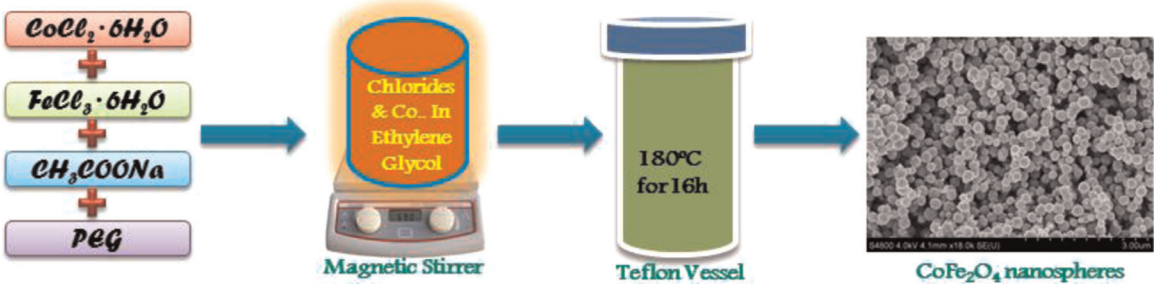

Fig. 1. Schematic diagram for hydrothermal synthesis of $CoFe_2O_4$ nanospheres.

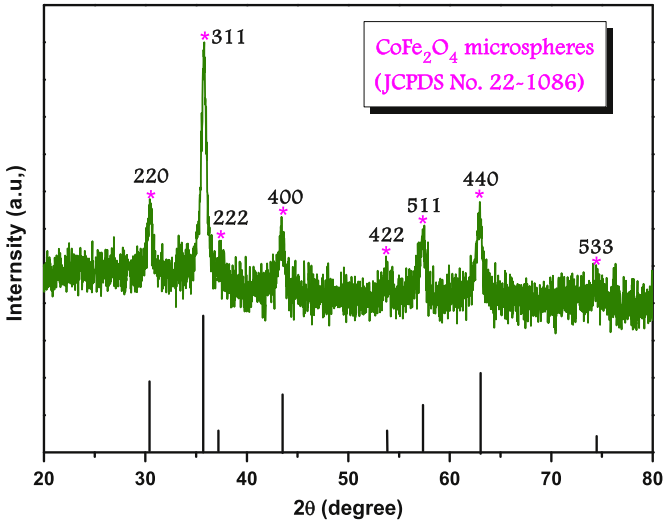

Fig. 2. XRD pattern of $CoFe_2O_4$ synthesized in EG solution.

vigorously stirred at 50 °C for 30 min to form a homogeneous solution. The transparent solution was then transferred into an autoclave, which was then tightly sealed and hydrothermally treated at 180 °C for 16 h in an oven. The mixture was allowed to cool to room temperature. The black product obtained was washed several times in excess water and dried at 60 °C for 6 h before characterization and application. The schematic diagram for hydrothermal synthesis of nanospheres is illustrated in Fig. 1.

The crystal structure of the synthesized powder was identified by a Bruker D2 X-ray diffractometer using Cu Kα radiation ($\lambda = 0.15405$ nm) in the range of 20–80 °C with step mode of 0.2/min. Field emission scanning electron microscopy (FESEM) was performed with a Hitachi S-4800 microscope coupled with an energy-dispersive X-ray spectrometer. Transmission electron microscopy (TEM) and high resolution transmission electron microscopy (HRTEM) characterizations were carried out on a Philips Tecnai F20 instrument working at 150 kV. Magnetization measurements of the samples were carried out using a physical properties measurement system at room temperature. FT-IR spectrum was recorded on a Perkin-Elmer V755 Fourier transform infrared spectrometer at wavenumbers 400–4000 cm^{-1} using KBr pellets. The surface area and the pore size were studied by nitrogen-sorption measurements which were performed on a Micromeritics ASAP 2020 gas sorptometer. Information about the oxidation states of these samples was obtained from X-ray Photoelectron Spectroscopy (XPS) using Kratos Analytical Axis Ultra DLD with Al $K\alpha_1$ source.

3. Results and discussion

After the precursor solution was heated at 180 °C for 16 h, the black powders were collected by a magnet. The structure and phase purity of the nanospheres were confirmed by X-ray diffraction patterns and is presented in Fig. 2. It can be seen that the diffraction peaks match well with the standard pattern of cubic $CoFe_2O_4$ with a spinel structure (JCPDS no. 22-1086). The peaks observed at 30.4°, 35.7°, 37.3°, 43.4°, 53.8°, 57.3°, 62.7°and 74.7° 2θ can be assigned to (220), (311), (222), (400), (422), (511), (440) and (533) planes of spinel $CoFe_2O_4$, respectively. The interesting observation is that broad peaks in Co ferrite indicate fine nanocrystalline nature of samples. The average crystal size of the mesoporous $CoFe_2O_4$ nanospheres calculated from the Scherrer equation was about 14.9 nm.

To analyze the nanoscale structure, both transmission and field-emission scanning electron microscopy (TEM/FESEM) were used. Fig. 3 shows SEM and TEM micrographs of mesoporous $CoFe_2O_4$ nanospheres. The typical low and high magnification FE-SEM images of $CoFe_2O_4$ are shown in Fig. 3(a) and (b). The SEM image of sample shows that the diameters of most of the spheres are in the range of 120–280 m. While, the TEM image (Fig. 3c) of sample shows that the diameters of most of the spheres are in the range of 90–180 nm. It can be seen the particle size distribution of nanoparticles on the surface of a sphere and the primary particle size is tens of nanometers. Fig. 3d shows the HRTEM image on the edge of a sphere, indicating the interplanar spacing of the parallel fringes was 0.266 nm at (220), which is in good agreement with the (220) plane of the spinel $CoFe_2O_4$. The EDX spectrum of $CoFe_2O_4$ shown in Fig. 3e demonstrates the presence of Co, Fe, and O with an approximate atomic ratio of 1:2:4, which is consistent with $CoFe_2O_4$. The percentage of Co/Fe values obtained is given in the inset of Fig. 3e.

The porous oriented ferrite nanospheres have shown good magnetic property. Fig. 4(a) presents the corresponding magnetization as a function of applied magnetic field, or the M versus H curve. The saturation magnetization (M_s) and the coercivity (H_c) of the cobalt ferrite nanospheres are about 60.19 emu/g and 136 Oe, which are lower to the values of bulk $CoFe_2O_4$ (80 emu/g and 150 Oe, respectively) [14]. The reduction in saturation magnetization may be attributed to the surface disorder or spin canting at the particles surface [15]. The center part of the Fig. 4a is enlarged and is shown in Fig. 4b. Keen observation of the Fig. 4b illustrates the ferromagnetic behavior of the powders.

The organic bonds present in mesoporous were characterized using the FTIR spectrum. Fig. 4c shows the FT-IR spectra of the $CoFe_2O_4$ nanospheres recorded between 4000 and 400 cm^{-1}. The absorption band (υ_1) around 600 cm^{-1} is attributed to stretching vibrations of tetrahedral complexes and band (υ_2) around 400 cm^{-1} to that of octahedral complexes [16,17]. The broad peak

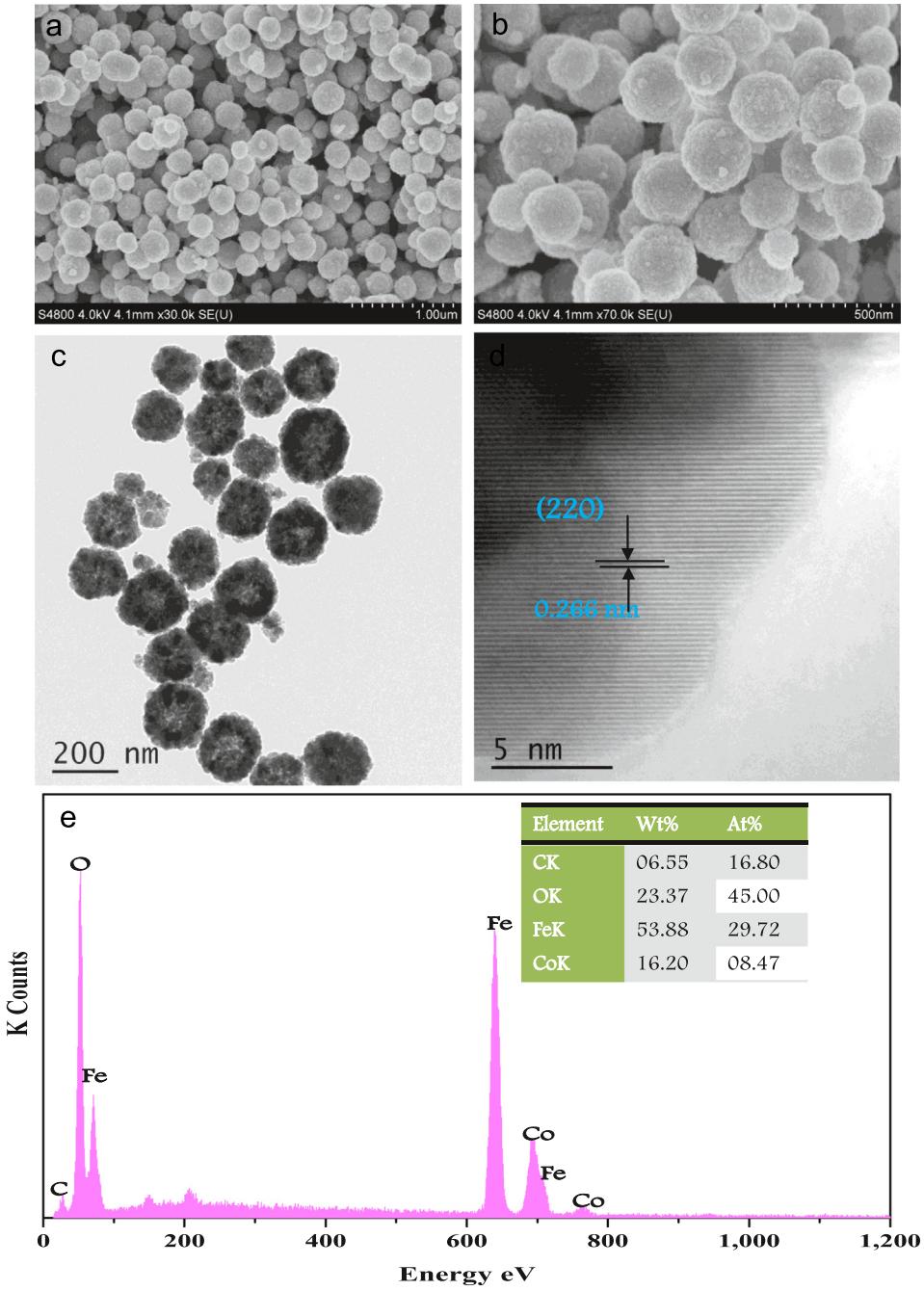

Fig. 3. SEM image (a and b), TEM image (c), HRTEM image (d) and EDX spectrum (e) of the $CoFe_2O_4$ nanospheres.

observed at ~3438 cm^{-1} is assigned to the stretching vibration of surface hydroxyls absorbed on surface and O-H groups in absorbed water, which indicates the presence of adsorbed moisture. The appearance of 2935 cm^{-1} waveband is assigned to the stretching of ether groups and the characteristics absorption of alkyl ($R\text{-}CH_2$) stretching modes. The peak observed at 1639 cm^{-1} is assigned to H-O-H bending vibration in water molecular. The weak peak at 1062 cm^{-1} is assigned to the C=O stretching.

Nitrogen adsorption–desorption studies on as-prepared mesoporous $CoFe_2O_4$ showed a type IV isotherm with an inflection of nitrogen adsorbed volume at P/P_0 about 0.5 (Fig. 4d) which confirmed the formation of mesoporous with a wormlike pore structure connected by tiny holes in the ferrite clusters. The specific surface area, calculated from the linear region of the Brunauer–Emmett–Teller (BET) plot, was 85.4 $m^2\,g^{-1}$. The pore-size distribution spectrum as shown in the inset of Fig. 4d, obtained by the Barrett–Joyner–Halenda method, clearly illustrated the presence of mesopores, which were mainly located in the narrow range of 5–20 nm, and peaked at 9 nm. In connection with the TEM image presented in Fig. 3c, such pores were (the enlarged edge of the microsphere) formed mainly from the stacking of nanoparticles.

The chemical composition of mesoporous $CoFe_2O_4$ nanospheres was further investigated by XPS. From Fig. 5a it can be clearly noticed that the peaks of Co, Fe, O and C exist. The C element (Fig. 5a) may originate from the adventitious carbon-based

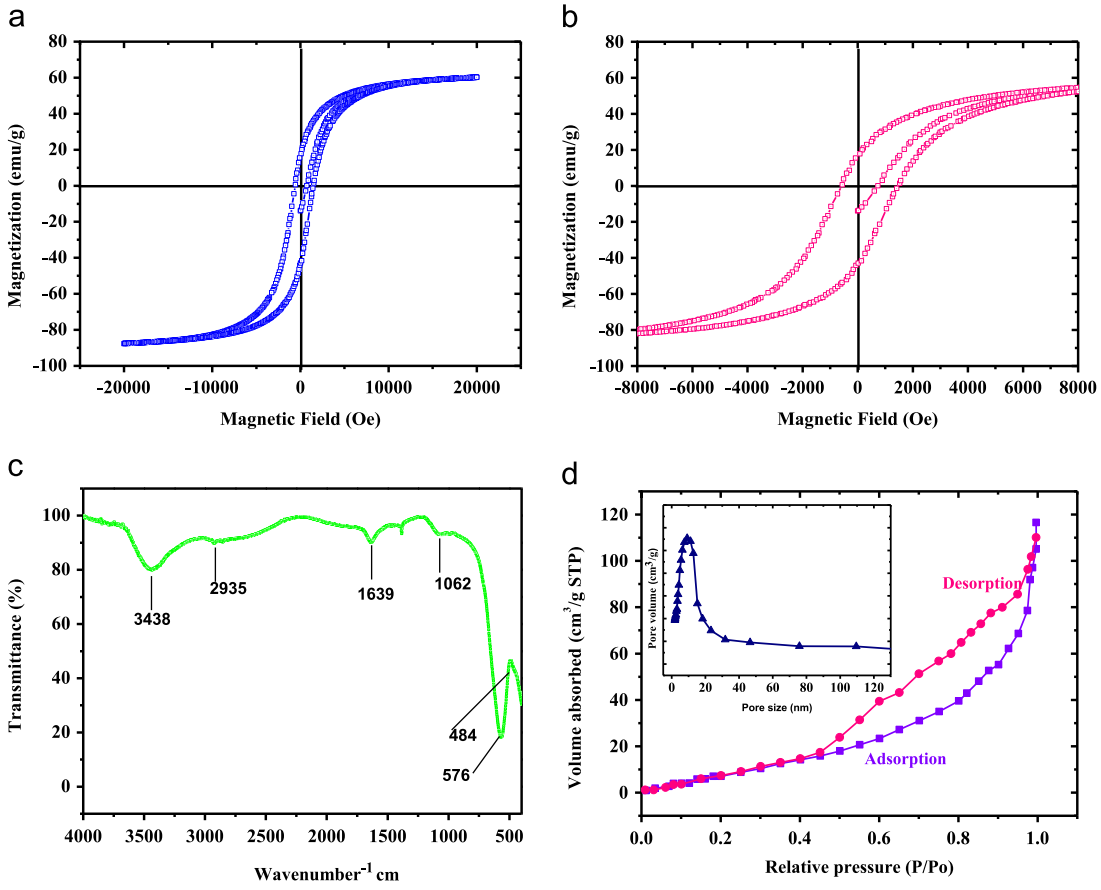

Fig. 4. *M–H* curves (a and b), FTIR (c) BET and pore-size distribution (inset) (d) of the $CoFe_2O_4$ nanospheres.

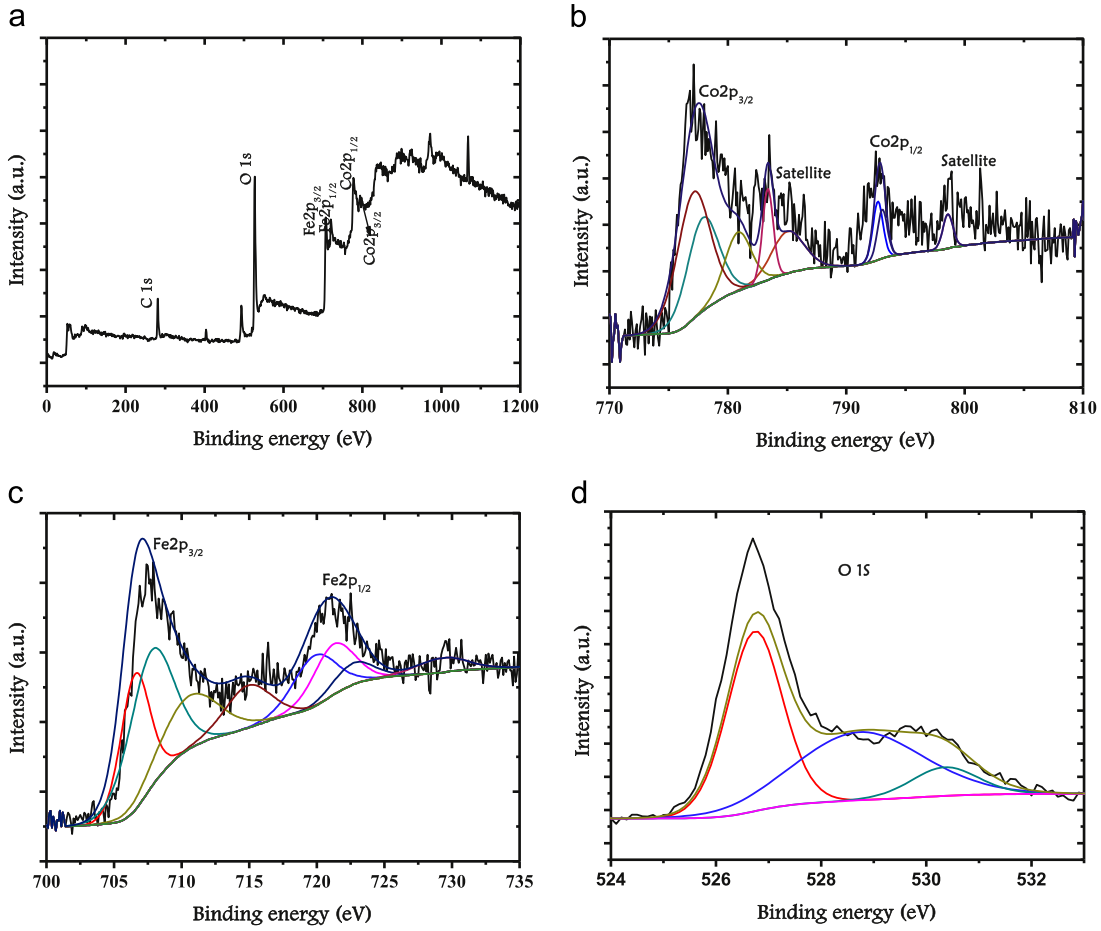

Fig. 5. (a) XPS fully scanned spectra of pristine $CoFe_2O_4$ nanospheres; high resolution XPS spectrum for (b) Co 2p, (c) Fe 2p and (d) O 1s.

contaminant and/or from the organic compounds such as residual ethylene glycol and PEG adsorbed on the surface. The binding energy of the C 1s peak at 284.8 eV is used as the reference for calibration. The peaks appearing at 777.3 and 792.5 eV correspond to the Co $2p_{3/2}$ and Co $2p_{1/2}$ states (Fig. 5b), indicating the presence of Co^{2+} [18]. Fig. 5c shows the Fe 2p spectrum. The Fe 2p shows two peaks at 708.96 and 722.5 eV which is consistent with Fe 2p binding energy for cobalt ferrite nanoparticles [19]. The peak located at 528.5 eV is attributed to the O 1s region [20], as shown in Fig. 5d.

In addition to the normal applications, such as constructing nanoscale magnetic devices and high-density storage media [21–23], the obtained porous magnetic micro/nanoospheres exhibits high specific surface areas and strong magnetic properties which could be used as an effective adsorbent for removal of some toxic chemicals. Generally, these chemicals are difficult to remove and are also important in environment remediation.

4. Conclusions

In this study, mesoporous $CoFe_2O_4$ nanospheres were prepared using a facile hydrothermal technique. The developed approach is simple and efficient route to fabricate cobalt ferrite nanospheres with a tunable diameter range of 120–180 nm. Information from the XRD pattern and FTIR spectrum of the mesoporous $CoFe_2O_4$ confirmed well with each other. EDX pattern confirmed the phase purity. As observed in XPS, cobalt was found to be in the 2^+ oxidation state and iron was found to be in the 3^+ oxidation state on the surface in cobalt ferrite sample, respectively. These cobalt ferrite porous microspheres have excellent magnetic properties and high surface area. The maximum saturation magnetization value of the product is 60.19 emu/g. The prepared products will have potential applications in many fields such as catalysis, lithium ion batteries and drug delivery, etc. This method provided a more convenient, one-step and economic way for scalable production of metal nanospheres.

References

[1] G. Liao, S. Chen, X. Quan, Y. Zhang, H. Zhao, Remarkable improvement of visible light photocatalysis with PANI modified core–shell mesoporous TiO_2 microspheres, Appl. Catal. B 102 (2011) 126–131.

[2] C. Knofel, V. Hornebecq, P.L. Llewellyn, Microcalorimetric investigation of high- surface-area mesoporous titania samples for CO_2 adsorption, Langmuir 24 (2008) 7963–7969.

[3] A. Manuel, G. Marta, N. Nuria, T. Carlos, M. Clara, M.R. Ibarra, S. Jesus, Development of magnetic nanostructured silica-based materials as potential vectors for drug-delivery applications, Chem. Mater. 18 (2006) 1911–1919.

[4] H. Tian, L. Hu, C. Zhang, S. Chen, J. Sheng, L. Mo, W. Liu, S. Dai, Enhanced photovoltaic performance of dye-sensitized solar cells using a highly crystallized mesoporous TiO_2 electrode modified by boron doping, J. Mater. Chem. 21 (2011) 863–868.

[5] Z. Li, J.C. Barnes, A. Bosoy, J.F. Stoddart, J.I. Zink, Mesoporous silica nanoparticles in biomedical applications, Chem. Sov. Rev. 41 (7) (2012) 2590–2605.

[6] X.Y. Yang, X.Y. Zhang, Y.F. Ma, Y. Huang, Y.S. Wang, Y.S. Chen, Superparamagnetic graphene oxide–Fe_3O_4 nanoparticles hybrid for controlled targeted drug carriers, J. Mater. Chem. 19 (2009) 2710–2714.

[7] H.P. Cong, J.J. He, Y. Lu, S.H. Yu, Water-soluble magnetic-functionalized reduced graphene oxide sheets: in situ synthesis and magnetic resonance imaging applications, Small 6 (2010) 169–173.

[8] C. Han, D. Zhao, C. Deng, K. Hu, A facile hydrothermal synthesis of porous magnetite microspheres, Mater. Lett. 70 (2012) 70–72.

[9] L.X. Yang, F. Wang, Y.F. Meng, Q.H. Tang, Z.Q. Liu, Fabrication and characterization of manganese ferrite nanospheres as a magnetic adsorbent of chromium, J. Nanomater. 293464 (2013) 5.

[10] J. Wanga, F. Ren, R. Yia, A. Yana, G. Qiua, X. Liua, Solvothermal synthesis and magnetic properties of size-controlled nickel ferrite nanoparticles, J. Alloy. Compd. 479 (2009) 791–796.

[11] Y.L. Wang, Y.N. Xia, Bottom-up and top-down approaches to the synthesis of monodispersed spherical colloids of low melting-point metals, Nano Lett. 4 (2004) 2047–2050.

[12] F. Caruso, M. Spasova, A. Susha, M. Giersig, R.A. Caruso, Magnetic nanocomposite particles and hollow spheres constructed by a sequential layering approach, Chem. Mater. 13 (2001) 109–116.

[13] K. Woo, J. Hong, S. Choi, H. Lee, J. Ahn, C.S. Kim, S.W. Lee, Easy synthesis and magnetic properties of iron oxide nanoparticles, Chem. Mater. 16 (2004) 2814–2818.

[14] M. Grigorova, H.J. Blythe, V. Rusanov, V. Petkov, V. Masheva, D. Nihtianova, L.M. Martinez, J.S. Munoz, M. Mikhov, Magnetic properties and mossbauer spectra of nanosized $CoFe_2O_4$ powders, J. Magn. Magn. Mater. 183 (1998) 163–172.

[15] C.R. Lin, Y.M. Chu, S.C. Wang, Magnetic properties of magnetite nanoparticles prepared by mechanochemical reaction, Mater. Lett. 60 (2006) 447–450.

[16] R. Kalai Selvan, C.O. Augustin, L.J. Berchmans, R. Saraswathi, Combustion synthesis of $CuFe_2O_4$, Mater. Res. Bull. 38 (2003) 41–54.

[17] M.A. Gabal, Y.M. Al Angari, M.W. Kadi, Structural and magnetic properties of nanocrystalline $Ni_{1-x}Cu_xFe_2O_4$ prepared through oxalates precursor, Polyhedron 30 (2011) 1185–1190.

[18] G. Zhou, D.K. Lee, Y.H. Kim, C.W. Kim, Y.S. Kang, Preparation and spectroscopic characterization of ilmenite-type $CoTiO_3$ nanoparticles, Bull. Korean Chem. Soc. 27 (2006) 368–372.

[19] H. Kim, D.H. Seo, H. Kim, I. Park, J. Hong, K.Y. Park, K. Kang, Multicomponent effects on the crystal structures and electrochemical properties of spinel-structured M_3O_4 (M=Fe, Mn, Co) anodes in lithium rechargeable batteries, Chem. Mater. 24 (2012) 720–725.

[20] L. Xue, C.B. Zhang, H. He, Y. Teraoka, Catalytic decomposition of N_2O over CeO_2 promoted Co_3O_4 spinel catalyst, Appl. Catal. B 75 (2007) 167–174.

[21] M. Sanjay, B. Sven, W. Ulf, H.R. Francisco, R.R. Albert, Chemical vapor growth of one-dimensional magnetite nanostructures, Adv. Mater. 20 (2008) 1550–1554.

[22] M.T. Chang, L.J. Chou, C.H. Hsieh, Y.L. Chueh, Z.L. Wang, Y. Murakami, D. Shindo, Magnetic and electrical characterizations of halfmetallic Fe_3O_4 nanofibers, Adv. Mater. 19 (2007) 2290–2294.

[23] C.J. Jia, L.D. Sun, F. Luo, X.D. Han, et al., Large-scale synthesis of single-crystalline iron oxide magnetic nanorings, J. Am. Chem. Soc. 130 (2008) 16968–16977.